

POTENTIAL INUNDATION DUE TO RISING SEA LEVELS IN THE SAN FRANCISCO BAY REGION

A Paper From:
California Climate Change Center

Prepared By:
Noah Knowles
U.S. Geological Survey

DISCLAIMER

This paper was prepared as the result of work sponsored by the California Energy Commission (Energy Commission) and the California Environmental Protection Agency (Cal/EPA). It does not necessarily represent the views of the Energy Commission, Cal/EPA, their employees, or the State of California. The Energy Commission, Cal/EPA, the State of California, their employees, contractors, and subcontractors make no warrant, express or implied, and assume no legal liability for the information in this paper; nor does any party represent that the uses of this information will not infringe upon privately owned rights. This paper has not been approved or disapproved by the California Energy Commission or Cal/EPA, nor has the California Energy Commission or Cal/EPA passed upon the accuracy or adequacy of the information in this paper.

DRAFT PAPER



Arnold Schwarzenegger, *Governor*



March 2009
CEC-500-2009-023-D

Acknowledgments

Thanks to David Schoellhamer and Bruce Jaffe for very helpful feedback, to Mick van der Wegen for performing Delft 3D test runs, and to the reviewers for helping improve the manuscript. This work was funded by the California Energy Commission's Public Interest Energy Research (PIER) Program through the California Climate Change Center at Scripps Institution of Oceanography, and by the CALFED Science Program CASCaDE Project.

Preface

The California Energy Commission's Public Interest Energy Research (PIER) Program supports public interest energy research and development that will help improve the quality of life in California by bringing environmentally safe, affordable, and reliable energy services and products to the marketplace.

The PIER Program conducts public interest research, development, and demonstration (RD&D) projects to benefit California's electricity and natural gas ratepayers. The PIER Program strives to conduct the most promising public interest energy research by partnering with RD&D entities, including individuals, businesses, utilities, and public or private research institutions.

PIER funding efforts focus on the following RD&D program areas:

- Buildings End-Use Energy Efficiency
- Energy-Related Environmental Research
- Energy Systems Integration
- Environmentally Preferred Advanced Generation
- Industrial/ Agricultural/ Water End-Use Energy Efficiency
- Renewable Energy Technologies
- Transportation

In 2003, the California Energy Commission's PIER Program established the **California Climate Change Center** to document climate change research relevant to the states. This center is a virtual organization with core research activities at Scripps Institution of Oceanography and the University of California, Berkeley, complemented by efforts at other research institutions. Priority research areas defined in PIER's five-year Climate Change Research Plan are: monitoring, analysis, and modeling of climate; analysis of options to reduce greenhouse gas emissions; assessment of physical impacts and of adaptation strategies; and analysis of the economic consequences of both climate change impacts and the efforts designed to reduce emissions.

The California Climate Change Center Report Series details ongoing center-sponsored research. As interim project results, the information contained in these reports may change; authors should be contacted for the most recent project results. By providing ready access to this timely research, the center seeks to inform the public and expand dissemination of climate change information, thereby leveraging collaborative efforts and increasing the benefits of this research to California's citizens, environment, and economy.

For more information on the PIER Program, please visit the Energy Commission's website www.energy.ca.gov/pier/ or contract the Energy Commission at (916) 654-5164.

Table of Contents

Preface..	iii
Abstract	vii
1.0 Introduction	1
2.0 Data and Methods	2
2.1. Method Overview	2
2.2. Elevation Data	2
2.3. Hydrodynamic Model Configuration and Validation.....	4
2.4. Hydrodynamic Model Inputs	5
2.5. Analysis	8
3.0 Results	10
4.0 Discussion.....	17
5.0 References.....	18
6.0 Glossary.....	20

List of Figures

- Figure 1. Sources of elevation data. Horizontal resolutions of original data are given in parentheses. All datasets were resampled to 2 m and merged.**Error! Bookmark not defined.**
- Figure 2. Key sites and features relevant to configuration and validation of TRIM-2D. The model grid is in gray. Gauge sites whose elevation relative to NAVD88 is known are in red. Gauges with data covering the validation period 1996–2007 are in bright blue. The two gauges whose data are used to derive conditions at the model boundaries (dashed blue lines) are in black squares.5
- Figure 3. Annual global mean surface air temperatures (red) from the CCSM3-A2 GCM run, and corresponding relative sea level rise (blue) from the Rahmstorf model.....6
- Figure 4. Hourly water levels at the Presidio for a typical year (2006), showing average historical (1900–2000) daily, monthly, and yearly high water levels6
- Figure 5. Areas inundated or vulnerable to inundation by average yearly Bay high-water levels as of 2000 (blue), and as of 2099 under a projected 139 cm sea level rise (red) 11
- Figure 6. Bay-average water level (upper) and total area around San Francisco Bay vulnerable to inundation (lower) versus return interval for four values of sea level rise projected over the next century. Relative sea level rise values are given in the legend in parentheses; the corresponding year in the CCSM3-A2 scenario is also given in the legend. 12
- Figure 7. Total area around San Francisco Bay vulnerable to yearly inundation for a range of sea level rise, broken down into land-cover categories..... 13
- Figure 8. Land-cover types of areas vulnerable to yearly inundation as of 2099 under a projected 139 cm sea level rise..... 14
- Figure 9. North Bay areas inundated or vulnerable to inundation by average yearly high water levels for present-day and projected 2100 conditions 15
- Figure 10. Central and South Bay areas inundated or vulnerable to inundation by average yearly high water levels for present-day and projected 2100 conditions 16

Abstract

An increase in the rate of sea level rise is one of the primary impacts of projected global climate change. To assess potential inundation associated with a continued acceleration of sea level rise, the highest resolution elevation data available were assembled from various sources and mosaicked to cover the land surfaces of the San Francisco Bay region. Next, to quantify high water levels throughout the Bay, a hydrodynamic model of the San Francisco Estuary was driven by a projection of hourly water levels at the Presidio. This projection was based on a combination of climate model outputs and empirical models and incorporates astronomical, storm surge, El Niño, and long-term sea level rise influences.

Based on the resulting data, maps of areas vulnerable to inundation were produced, corresponding to specific amounts of sea level rise and recurrence intervals. These maps portray areas where inundation will likely be an increasing concern. In the North Bay, wetland survival and developed fill areas are at risk. In Central and South bays, a key feature is the bay-ward periphery of developed areas that would be newly vulnerable to inundation. Nearly all municipalities adjacent to South Bay face this risk to some degree. For the Bay as a whole, as early as 2050 under this scenario, the one-year peak event nearly equals the 100-year peak event in 2000. Maps of vulnerable areas are presented and some implications discussed.

Keywords: sea level rise, climate change, estuary, San Francisco Bay, flooding

1.0 Introduction

An increase in the rate of rise of mean sea level is one of the primary and potentially most troublesome aspects of projected climate change. Sea level at San Francisco's Presidio tide gauge has risen at a rate of 22 centimeters (cm) per century over the last century (Flick 2003), consistent with global average rates in recent decades (Church et al. 2004). Church and White (2006) found that the rate of global sea level rise in recent years increased significantly over that of the previous several decades. As global temperatures continue to warm, sea level will continue to rise in response, probably at a greater rate than observed historically. While it is generally accepted that global climate warming will increase rates of sea level rise, the range in estimated rates is wide, mainly due to the uncertainty in the amount of meltwater from land-based ice in Greenland and Antarctica. Recent projections (Rahmstorf 2007) estimate the range of increase of global sea level at 40–140 cm above recent levels. Another recent study (Pfeffer et al. 2008) produced a somewhat higher estimate (80–200 cm), reinforcing the opinion that sea level rise during the next several decades could exceed the estimates provided by the Intergovernmental Panel on Climate Change (IPCC) Third and Fourth Assessments (IPCC 2001, 2007). Concerning the high end of the range, Pfeffer et al. concluded that sea level rise is very unlikely to exceed 200 cm by 2100. Beyond 2100, however, sea levels are expected to continue to rise for several centuries due to oceanic thermal inertia (Wigley 2005).

Pioneering studies by Williams (1985, 1987) and Gleick and Maurer (1990) were the first to estimate the impacts of sea level rise in San Francisco Bay. Williams found that a 100 cm sea level rise would result in an inland shift of the estuarine salinity field of 10–15 kilometers (km), potentially threatening ecosystems and freshwater supplies. In their comprehensive effort, Gleick and Maurer estimated that a 100 cm sea level rise would result in losses of residential, commercial and industrial structures bordering the Bay valued at \$48 billion (1990 dollars).

A detailed assessment of what areas adjacent to the Bay are vulnerable to inundation due to projected sea level rise is necessary in development planning to avoid future risk, inform infrastructure planning (e.g., water treatment outflows and roadways), and design wetland restoration efforts with the ability to adapt to future changes, among many other uses. The present study uses hydrodynamic modeling in conjunction with the most accurate elevation data available to develop high-resolution maps of areas vulnerable to periodic inundation corresponding to varying amounts of sea level rise, along with statistical descriptions of the frequency of the potential inundation. The data are publicly available for use in other efforts at <http://cascade.wr.usgs.gov>.

This study addresses only the question of which areas are vulnerable to inundation, as opposed to quantifying the actual risk of inundation under a future scenario. No distinction is made between vulnerable areas already protected by levees and those that are not—at the time of this study, insufficient data on levees were available to make this distinction. Thus, potential improvements to existing levees or construction of new levees are not considered. Where levees currently exist, the results presented below indicate areas that would be flooded if these levees were to fail (due to, for example, a high-water event or an earthquake). Also, shoreline erosion and the potential accumulation of sediment and organic matter with sea level rise are not accounted for here. As levee data become available and as modeling capabilities improve, future studies will address such issues and directly evaluate possible mitigation actions.

In the following sections, the elevation dataset and hydrodynamic modeling approach used are described. Then some key results, including maps and analysis of areas vulnerable to periodic inundation are presented. Finally, implications of the results, important caveats, and future directions for this work are discussed.

2.0 Data and Methods

2.1. Method Overview

This study uses a hydrodynamic model to simulate water levels throughout San Francisco Bay under conditions of projected sea level rise through 2100. Statistical analysis of the projected water levels provides characterization of both long-term trends in mean sea level and high water levels associated with short-term variability at points along the Bay's shoreline. These high water levels are then compared to nearby land-surface elevations to determine areas vulnerable to inundation around the Bay.

2.2. Elevation Data

As the foundation of this study, the highest resolution elevation data available to date were assembled and mosaicked to cover the entire region. This new dataset necessarily represents a patchwork of LiDAR (light detection and ranging) data from multiple sources, photogrammetry data, and IfSAR (interferometric synthetic aperture radar) data where no better data were available. This dataset contains elevation data from five sources (Figure 1):

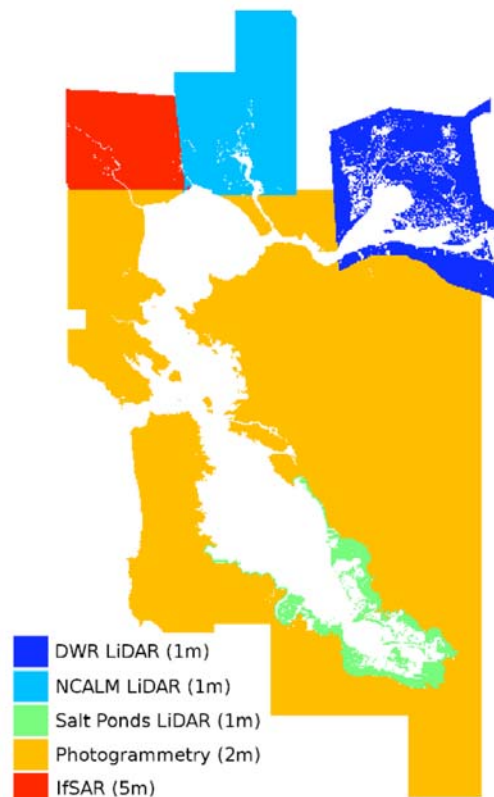


Figure 1. Sources of elevation data. Horizontal resolutions of original data are given in parentheses. All sources have a vertical uncertainty of 10-40 cm RMSE, except IfSAR, which has an uncertainty of 100 cm RMSE. All datasets were resampled to 2 m and merged.

1. Sacramento-San Joaquin Delta Region LiDAR dataset, produced by the California Department of Water Resources from missions flown in 2007 and 2008. The dataset's horizontal resolution is 1 meter (m).
2. Napa watershed LiDAR from the University of California at Berkeley Data Distribution Center for the National Center for Airborne Laser Mapping (NCALM). These data are from flights in 2003, and the horizontal resolution is 1 m.
3. South Bay salt ponds LiDAR data (Foxgrover and Jaffe 2005). These data are from flights in 2004, and the horizontal resolution is 1 m.
4. San Francisco region photogrammetric elevation data. The U.S. Geological Survey (USGS), in cooperation with the National Geospatial-Intelligence Agency (NGA), developed ground elevation data from flights in 2003 at a horizontal resolution of 2 m for the purpose of producing orthorectified images. We assembled the tiles of elevation data and adjusted them to the North American Vertical Datum of 1988 (NAVD88) datum using the GEOID03 model, resulting in a dataset covering the greater Bay-Delta region (Coons et al. 2008). The Delta/Suisun Bay portion of the USGS/NGA dataset has since been superseded by the Delta LiDAR dataset.
5. Intermap IfSAR data. Since the above data sources left a gap in the Petaluma River and Sonoma Creek watersheds, the Intermap data, produced using synthetic aperture radar methods, were obtained. These data are not ideal, as they have a 5 m horizontal posting and 1 m root mean square error (RMSE) vertically. However, at the time of this writing they are the most accurate data available for that area.

All elevation data were referenced to NAVD88 in the Universal Transverse Mercator projection (zone 10). Where necessary, the conversion to NAVD88 was made using the GEOID03 model (www.ngs.noaa.gov/PC_PROD/GEOID03).

These five datasets were joined after comparison in areas of overlap. Agreement between all overlapping datasets was good, with slight positive biases (10–20 cm) of the photogrammetry relative to the LiDAR datasets. This bias makes sense as the LiDAR data are typically “bare-ground” elevations, whereas the photogrammetry data include the height of vegetation. As such any estimates of inundation vulnerability in areas covered by the photogrammetry dataset may be considered conservative. All datasets were resampled to a common horizontal resolution of 2 m using the nearest-neighbor method, then merged.

The last step in developing the regional elevation dataset was to mask out open water, as none of the measurement methods described above produce reliable results over water. Three separate water masks were used in this process. Outside the mouth of San Francisco Bay, the shoreline was extracted from the National Oceanic and Atmospheric Administration (NOAA) National Shoreline dataset (shoreline.noaa.gov/data/datasheets). Inside the Bay, another dataset was available—a shoreline coverage extracted from the San Francisco Estuary Institute (SFEI) EcoAtlas (www.sfei.org/ec atlas). The SFEI and NOAA shoreline datasets were

checked against 2003 orthoimages, and it was qualitatively determined that the SFEI shoreline was more accurate. The two shorelines were clipped and joined at the Golden Gate. They are both representative of the mean high water (MHW) tidal datum. Finally, Foxgrover (2005) generated a water mask for the South Bay LiDAR data based on return characteristics that was used to mask open water in the part of the Bay covered by that dataset.

The LiDAR and photogrammetry elevation data have vertical accuracies of 10–40 cm RMSE and, as of this writing, the assembled dataset represents the most accurate elevation data publicly available (excluding the IfSAR data which are under a restrictive license) covering this region.

2.3. Hydrodynamic Model Configuration and Validation

To assess what land elevations around the Bay are vulnerable to periodic inundation, estimates of high water levels throughout the Bay must be generated. These high water excursions are the result of tides, storm surge, and other dynamic processes, requiring the use of a hydrodynamic model for this task. This model will be used to produce a single 100-year projection of hourly water levels throughout the Bay for use in the subsequent analysis. TRIM-2D (Cheng et al. 1993) is a numerical model that uses a semi-implicit finite-difference method for solving the two-dimensional shallow-water equations in San Francisco Bay. The model uses a 200 m horizontal grid with nearly 50,000 grid cells and is configured here with a six-minute time step. It is driven solely by water level time series at its seaward and landward boundaries, which are translated in phase and amplitude from the tide gauges with sufficiently long records nearest these boundaries, namely the Presidio and Port Chicago stations (Figure 2). Cheng et al. (1993) demonstrated that the TRIM-2D hydrodynamic model accurately reproduces the historical amplitudes and phases of tidal constituents throughout the Bay.

The TRIM-2D model was chosen because it is capable of performing the century-long simulation needed to address the effects of long-term climate change in a reasonable amount of time. While the ideal model for this study would have a boundary condition much farther upstream than Port Chicago to avoid boundary issues and would directly simulate the hydrodynamics of inundated areas, such a model is not yet publicly available. Those proprietary models which do include these features are currently too computationally demanding to perform the needed runs in a reasonable amount of time.

The TRIM-2D model in its native configuration simulates water levels relative to mean lower-low water (MLLW), but water levels relative to NAVD88 are needed here. The model takes as input a datum file, which was previously configured relative to the MLLW tidal datum. By adjusting this file appropriately, the model can be reconfigured to generate output water heights relative to NAVD88. To accomplish this reconfiguration, heights of MLLW relative to NAVD88 from 15 leveled tide gauges throughout the Bay (Figure 2) were obtained from NOAA (tidesandcurrents.noaa.gov). These heights were then interpolated using the method of regular splines with tension (Mitasova and Hofierka 1993) to produce a MLLW adjustment grid. This grid was used in the new input datum file to TRIM-2D, and the resulting simulated water heights are thereby referenced to NAVD88.

With the model adjusted to the correct datum, the calibration coefficients used to translate the boundary forcings from the nearby tide gauges to the model boundaries needed to be retuned.

To this end, the model was run repeatedly over the period 1996–2007. This validation period was chosen because hourly water level observations at six sites throughout the Bay (Figure 2), including the gauges used to generate the boundary conditions, were available for the full period. The calibration coefficients were iteratively adjusted to minimize differences between simulated and observed mean sea level and average daily tidal range at these six sites.

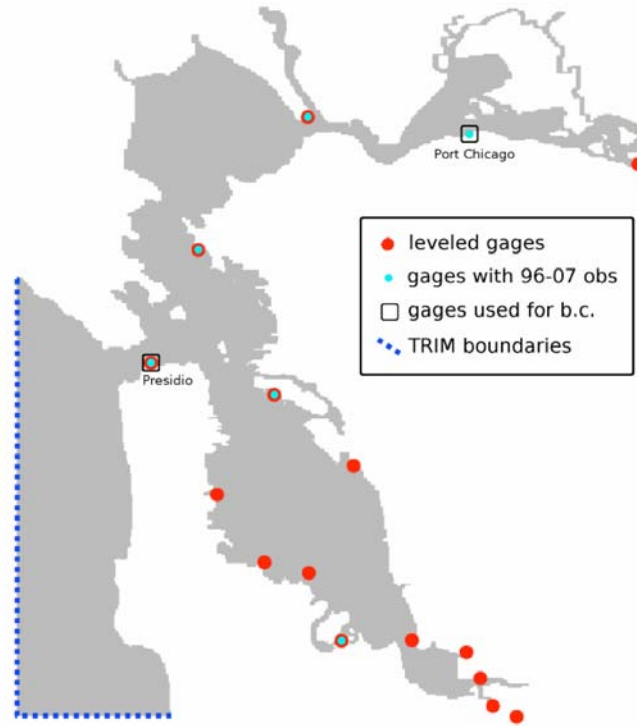


Figure 2. Key sites and features relevant to configuration and validation of TRIM-2D. The model grid is in gray. Gauge sites whose elevation relative to NAVD88 is known are in red. Gauges with data covering the validation period 1996–2007 are in bright blue. The two gauges whose data are used to derive conditions at the model boundaries (dashed blue lines) are in black squares.

2.4. Hydrodynamic Model Inputs

TRIM-2D requires two time series as inputs—water levels at six-minute intervals at the Presidio and Port Chicago sites—which are then mapped using calibrated coefficients to serve as the model's boundary conditions (Figure 2). A 100-year projection of mean sea level at the Presidio location was produced by Cayan et al. (2009) using the method of Rahmstorf (2007), based on global mean temperatures as projected by the CCSM3 global climate model (www.cesm.ucar.edu) under the A2 greenhouse gas emissions scenario (Figure 3). This model projects a $\sim 4.5^{\circ}\text{C}$ ($\sim 8.1^{\circ}\text{F}$) increase in global average surface air temperatures by 2100. This is a relatively high (but not the highest) amount of warming among the ensemble of IPCC Fourth Assessment model results (IPCC 2007). Using the Rahmstorf method, this warming corresponds to a 139 cm rise in mean sea level.

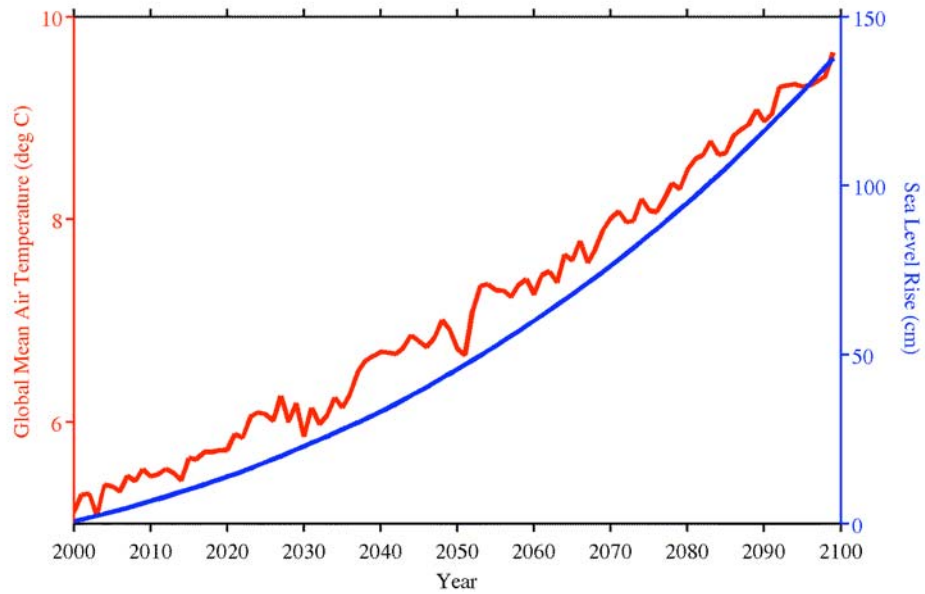


Figure 3. Annual global mean surface air temperatures (red) from the CCSM3-A2 GCM run, and corresponding relative sea level rise (blue) from the Rahmstorf model

This method provided the secular trend in water levels at the Presidio, but water levels vary under the influence of several forces over multiple time scales. Astronomical tides, storm surges, and El Niños are all major contributors to water level variability. The result of these and other forces is that water levels reach successively higher peak water levels at longer time scales. Figure 4 illustrates average the historical (1900–2000) average daily, monthly, and yearly high water levels compared to hourly data for a typical year (2006) at the Presidio.

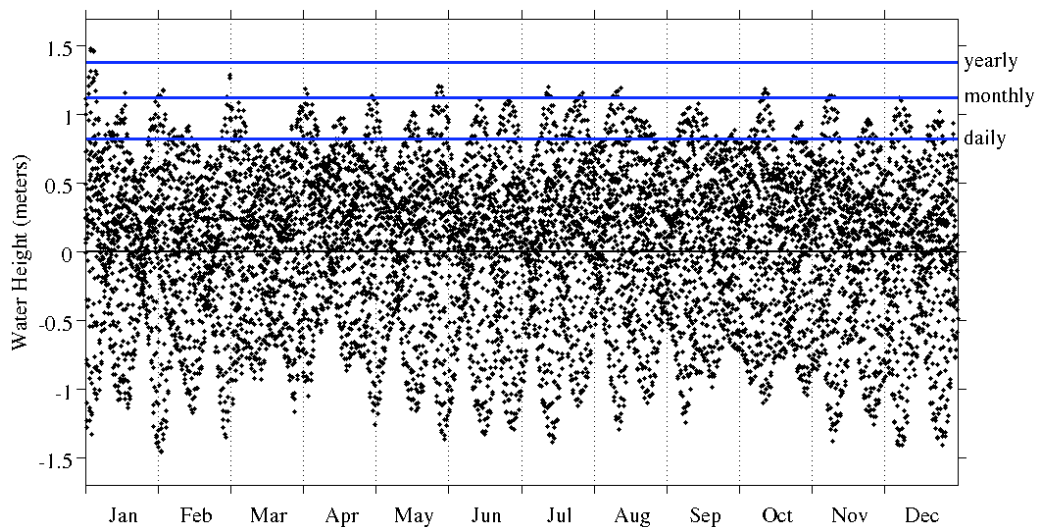


Figure 4. Hourly water levels at the Presidio for a typical year (2006), showing average historical (1900–2000) daily, monthly, and yearly high water levels

To incorporate this variability into the projected water level time series, historical variability was superposed on the projected long-term trend in mean sea level. To do this, hourly water level data (1900–1999) from the Presidio gauge were detrended using a least-squares linear fit to remove any historical sea level rise signal. A few small gaps in the historical data were filled using hindcast astronomical tides (Cheng and Gartner 1984). The resulting 100-year detrended time series, which contains variability over a range of periods ranging from tidal to decadal scales, was added to the secular trend provided by Cayan to produce a 100-year projection of hourly water levels at the Presidio. This use of historical short-term variability (defined here as any variability other than the long-term trend) to represent future short-term variability assumes two things—first, that the probability distribution of short-term variability will remain unchanged under the climate change projections, and second, that these short-term variations and the secular component of the water level time series at the Presidio site are linearly superposable. Cayan et al. (2008) found the first of these assumptions to be true. The second follows as a reasonable approximation from the fact that the amplitude of both components— $O(1\text{ m})$ —is considerably smaller than the average depth near the Presidio site— $O(100\text{ m})$. This is because in sufficiently deep water, surface waves do not interact with the bottom and are thus unaffected by changes in mean depth.

With the first of the two required TRIM-2D input time series thus obtained, the Port Chicago time series was next produced. Lacking more than a few decades of data at the Port Chicago site, the approach used for the Presidio site was unworkable. The chosen solution was to map the Presidio time series to Port Chicago using a temporal version of the technique of constructed analogues (Hidalgo et al. 2008). In this approach, the historical water-level time series (1996–2007) at the two stations were used to create a “map” which generates a 100-year hourly water-level projection at Port Chicago based on the Presidio projection described above. Specifically, the Presidio projection was stepped through five days at a time, with the preceding and succeeding days included to make a week of data. Each of these seven-day periods was expressed as a linear combination of the 22 best-matching (using RMS error) seven-day periods from the historical Presidio record (22 was found to be the optimal number of matches). The same coefficients in this optimal linear combination were then applied to the corresponding seven-day periods from the historical Port Chicago record to produce the estimate of Port Chicago water levels for the corresponding projected five-day period, after dropping the first and last days (which were included to minimize boundary effects in the procedure). One constraint on the method is that matching weeks were restricted to the same quarter of the year as the target week, allowing some accounting of the influence of the annual cycle of storm surges and freshwater flow.

Stepping through the 100-year Presidio projection in this manner, a corresponding 100-year projection of hourly water levels was developed for the Port Chicago station. The described procedure was applied to the non-secular component of the Presidio projection, and the Rahmstorf secular trend was then added to the resulting Port Chicago time series. A more complete description of the original method (as applied to spatial fields instead of time series) is given in Hidalgo et al. (2008).

Projecting future Port Chicago water levels based on historical water levels assumes that amplitudes are unchanged as mean depth increases. Recent test runs using a Delft3D model of the Bay / Delta (Mick van der Wegen, personal communication) suggest that increasing mean sea

levels would result in increased tidal amplitudes at Port Chicago, meaning the results presented here are conservative, particularly in the landward reach of the estuary. These same test runs also indicate that any attenuation between the Presidio and Port Chicago sites of the long-term sea-level rise signal would be negligible, validating the method described above.

A validation run of the above procedure was performed, in which the historical Presidio record (1996–2007) was mapped to Port Chicago by excluding the target week from being selected as one of the matching patterns. The resulting “mapped” Port Chicago time series agreed well with the actual observed time series, with an RMS error of 6 cm (compared to an average daily tidal range of 148 cm) and a correlation coefficient of $r > 0.99$.

Both the Presidio and the Port Chicago 100-year hourly projections were interpolated from an hourly to a six-minute time step, and a week of hindcast astronomical tides were prepended to allow for model spin-up. A run of TRIM-2D was performed using these inputs (with a real-world run time of three weeks), resulting in a 100-year projection of 6-minute gridded water heights throughout San Francisco Bay corresponding to a sea level rise of 139 cm by 2100.

2.5. Analysis

Based on the projections of gridded water level time-series, water-height fields were developed corresponding to combinations of (1) specific amounts of sea level rise, and (2) specific return intervals (e.g., 100-year high water with 46 cm sea level rise). This was accomplished by first separating the water-level time series of each model grid cell into a long-term trend and a detrended short-term variability time series. The long-term trend was estimated as the optimal second-degree least-squares fit to the full time series, and the residual was the short-term variability. Using the parameters of the long-term fits, the bay-wide mean water-height field corresponding to any date in the century-long projection could then be determined, providing #1 above.

High water levels corresponding to specific return intervals associated with short-term variability were calculated next using the detrended time series at each grid cell. Return intervals represent the average period between events of a certain magnitude (corresponding to “return levels”), such as floods, and are widely used for a variety of purposes, such as design and planning, regulation, and insurance requirements. Return levels are determined by the application of the generalized extreme value distribution (GEV), formulated by Fisher and Tippett (1928). They showed that block maxima, or a series of maxima each calculated over a specific time interval (e.g., annual high water levels), are characterized by the cumulative distribution function given in Equation 1.

$$F(x; \hat{\mu}, \hat{\sigma}, \hat{\tau}) = \begin{cases} \exp \left\{ - \left[1 + \hat{\tau} \left(\frac{x - \hat{\mu}}{\hat{\sigma}} \right) \right] \frac{1}{\hat{\tau}} \right\}, & 1 + \hat{\tau} \left(\frac{x - \hat{\mu}}{\hat{\sigma}} \right) > 0 \\ \exp \left\{ - \exp \left[- \left(\frac{x - \hat{\mu}}{\hat{\sigma}} \right) \right] \right\}, & \hat{\tau} = 0 \end{cases} \quad \text{Eq. 1}$$

The cumulative distribution function of Equation 1 was fit to the annual maxima of the detrended time series in each grid cell throughout the Bay using the maximum-likelihood method,¹ also developed by Fisher. This resulted in values of the parameters μ , σ , and ξ for each grid cell. The most important of these parameters, ξ , is called the shape parameter and determines the shape of the extreme tail of the probability distribution of the process being characterized—in this case water level variability. For all points on the Bay grid, $\xi < 0$, representing a short-tailed process. This indicates relatively small differences between high-water levels for progressively longer return intervals. The inverse of Equation 1 was then used to determine water-level heights throughout the Bay for a given return interval, corresponding to a specific value of the cumulative distribution function.

Finally, for a specified date from 2000–2100 we can determine the gridded mean sea level for that date using the parameters describing the long-term trend. For a specified return interval we can determine the associated water-height field using the GEV parameters. Adding the two values allows the high-water levels of the Bay to be characterized, both probabilistically and through time for any combination of date and return interval.

This approach assumes that the simulated 100-year water-level time series can be separated into a long-term trend and short-term variability with the latter component being stationary (a requirement of the GEV analysis), thus extending to the entire Bay the assumption that the short-term variability is independent of the long-term trend. While this assumption was clearly reasonable near the deeper waters of the Presidio site, it is not obviously so in the shallower parts of the Bay where surface waves may interact with the bottom. To test this assumption, a separate hydrodynamic simulation was carried out in which the long-term sea level trend was removed from the boundary conditions, leaving only the short-term component. The last few years of the 100-year projection were simulated in this manner, and the results were compared to the detrended signal derived from the output of the original simulation. If short-term variability is indeed independent of the long-term trend in mean sea level, the two should be identical. The test run showed very slightly higher peak water levels—O(1 cm)—in most of the Bay, indicating that short-term variability is dampened negligibly by the increase in mean depth with sea level rise, justifying the approach used here.

Importantly, an unintended benefit of this approach is that the results are not limited to the particular climate scenario used (in this case, CCSM3-A2). That is, the results are not dependent on time elapsed in the scenario but instead on the specific amount of sea level rise that has occurred. By specifying this amount along with the statistics of the short-term variability (which, being stationary through time and across scenarios, are independent of the scenario chosen), the results are completely specified.

Using the approach described above, high-water levels were determined for different values of sea level rise and return interval for each of the nearly 50,000 points in the TRIM-2D 200 m horizontal grid. In particular, sea level rise values considered were 0 cm (corresponding to the year 2000), 46 cm (corresponding in the CCSM-A2 scenario to the year 2050), 100 cm (the year 2081), and 139 cm (the year 2099). These intervals were chosen because they were of particular

¹ All analysis and figures were produced using GRASS/QGIS, Matlab, and R statistical analysis software.

interest to various state and local agencies. For each of these cases, the inverse of Equation 1 was used to determine the high water levels corresponding to return intervals of 1, 10, 50, 100, and 500 years.

Finally, each water-height field was compared at all points along the Bay's shoreline to the adjacent land surface elevation data to assess what areas would be inundated (at least as often as the specified return interval, on average) by water at these heights, resulting in the inundation maps and data presented in the next section. A final dataset used to portray vulnerable areas in terms of land cover type (Figures 7 and 8) was the National Land Cover Dataset of 2001 (NLCD01, www.epa.gov/mrlc/nlcd-2001.html).

Again, the effect of present or future levees, potential accumulation of sediment and organic matter, and shoreline erosion are not included in this study. Further, attenuation of short-term variability over inundated areas has not been accounted for; therefore, vulnerability to inundation may be overstated for areas well removed from the Bay's (and the TRIM-2D model's) present-day shoreline. The estimates presented in this study have not taken into account the effect of wind waves on water levels, nor, in the long term, the possibility of tsunamis. Subsidence of the land surface may also exacerbate some of the vulnerabilities presented here; conversely, long-term uplift may do the opposite. The effect of high freshwater inflows on stage are accounted for, but only corresponding to historical climate; increased winter flood peaks associated with climate warming (e.g., Knowles and Cayan 2002) would likely produce greater inundation vulnerabilities than presented here, especially in the northern part of the estuary.

3.0 Results

Figure 5 shows areas whose elevations lie below the adjacent average yearly high water levels (i.e., one-year recurrence levels) under conditions of present mean sea level in blue, and under conditions of a 139 cm increase in mean sea level in red. For clarity, intermediate values of sea level rise are not shown in this and subsequent maps; for smaller values of sea level rise, the red areas would be smaller. Most of the areas indicated as vulnerable to inundation are presently behind levees and would only be inundated if those levees breached or were overtopped. Other areas indicated as vulnerable to inundation are presently wetlands that are inundated periodically by the tides. The northern and southern sections of the San Francisco Bay region are later addressed separately in more detail (Figures 9 and 10).

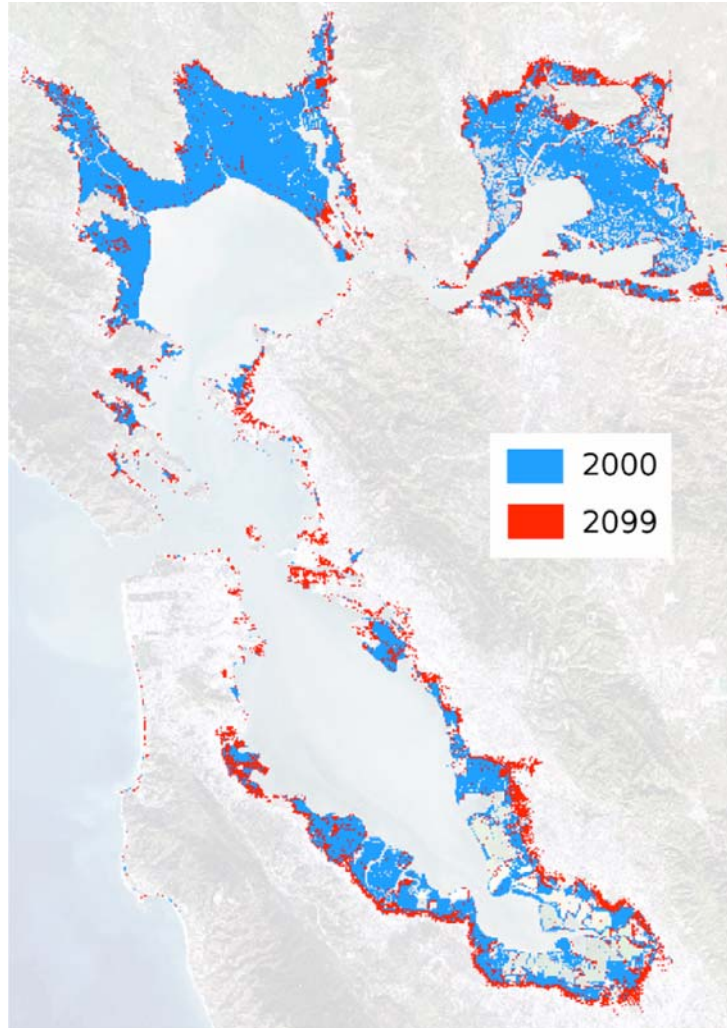


Figure 5. Areas inundated or vulnerable to inundation by average yearly Bay high-water levels as of 2000 (blue), and as of 2099 under a projected 139 cm sea level rise (red)

Figure 6 shows the bay-wide mean high-water levels and total area vulnerable to inundation for four values of sea level rise (0, 46, 100 and 139 cm) and five different return intervals (1, 10, 50, 100 and 500 years). As described earlier, water level variability in the Bay is a short-tailed process ($\kappa < 0$), evidenced here by the progressively flatter response of water level and vulnerable area with increasing return interval. It should be noted that the 500-year return levels should include the effects of a potential tsunami, but the evaluation of such effects is beyond the scope of the current investigation. Inclusion of tsunami effects would likely increase the 500-year return levels substantially. Still, the difference between the 10, 50, and 100-year return levels is much smaller than the projected magnitude of increase in mean sea level over the century. As early as 2050 under this scenario, the one-year peak event nearly equals the 100-year peak event in 2000.

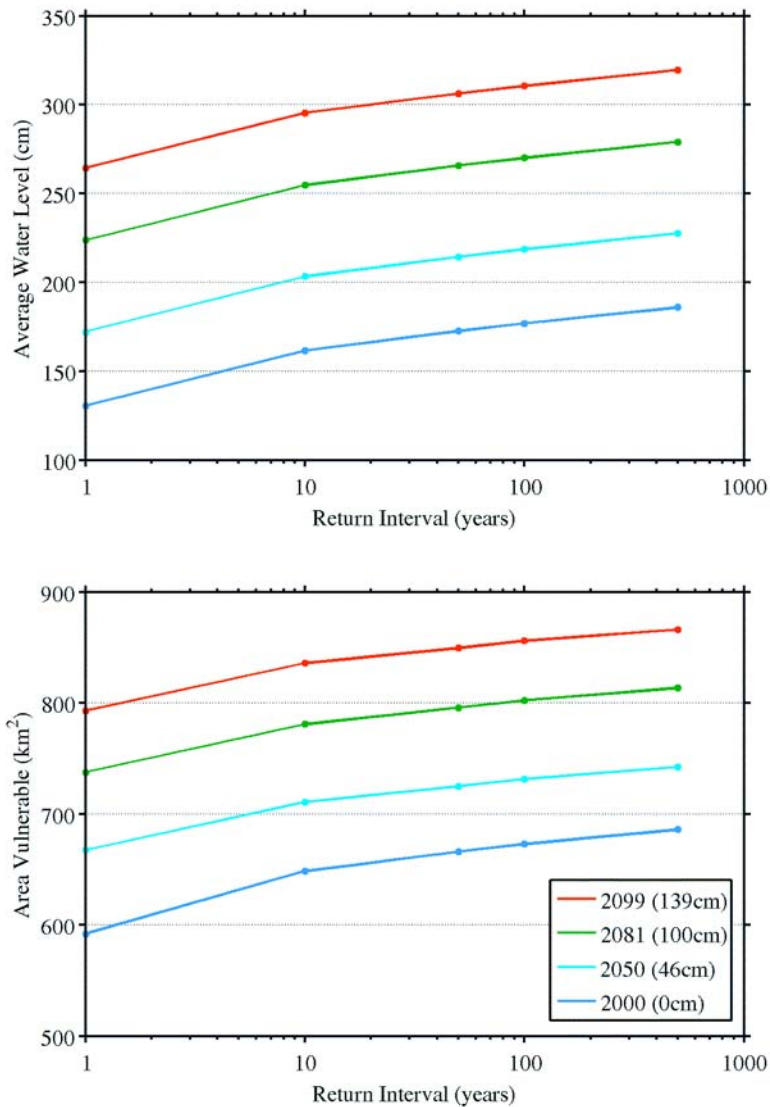


Figure 6. Bay-average water level (upper) and total area around San Francisco Bay vulnerable to inundation (lower) versus return interval for four values of sea level rise projected over the next century. Relative sea level rise values are given in the legend in parentheses; the corresponding year in the CCSM3-A2 scenario is also given in the legend.

To assess what types of land areas are vulnerable, Figures 7 and 8 show the areas vulnerable to periodic inundation, expressed in terms of land cover types based on the NLCD01 dataset. The dominant categories of land cover around San Francisco Bay are wetlands, grasslands, and developed areas. Wetlands, which are already partly intertidal, become more fully intertidally inundated and ultimately subtidal under sea level rise, although the issue of accretion's ability to keep pace with sea level rise is an unresolved research question. Grasslands (mostly grazed pasture) are typically already behind levees and sea level rise would increase the risk of overtopping or breaching those levees. The total area of vulnerable grassland changes little with sea level rise.

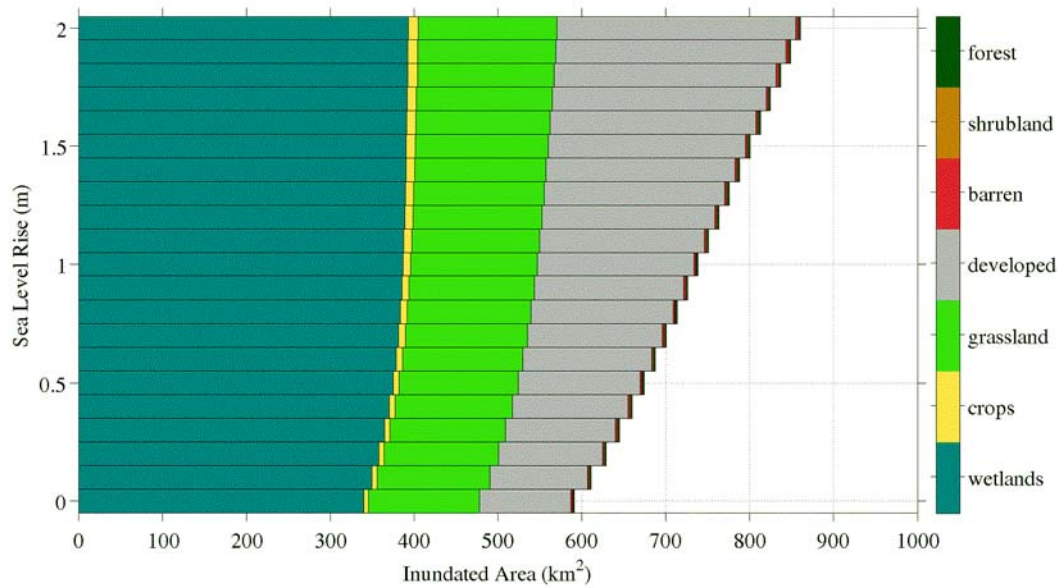


Figure 7. Total area around San Francisco Bay vulnerable to yearly inundation for a range of sea level rise, broken down into land-cover categories

Today, a total of about 590 square kilometers (km²) are periodically inundated or vulnerable to inundation, with 340 km² being existing wetlands, and 242 km² consisting of grasslands and developed areas already protected by levees. Under the 46 cm sea level rise projected by 2050 in the CCSM3-A2 scenario, the total vulnerable area increases by 13%, and under the 139 cm sea level rise projected by 2099, the total vulnerable area increases by 33% to 788 km². The largest change in area of a vulnerable land cover type occurs for developed areas. Vulnerable developed area more than doubles by 2099, from 109 km² to 225 km². These estimates assume no change in land-use assignments over time; it is possible that some of the land currently assigned to other categories will ultimately be developed, resulting in an even greater value for total vulnerable developed area.

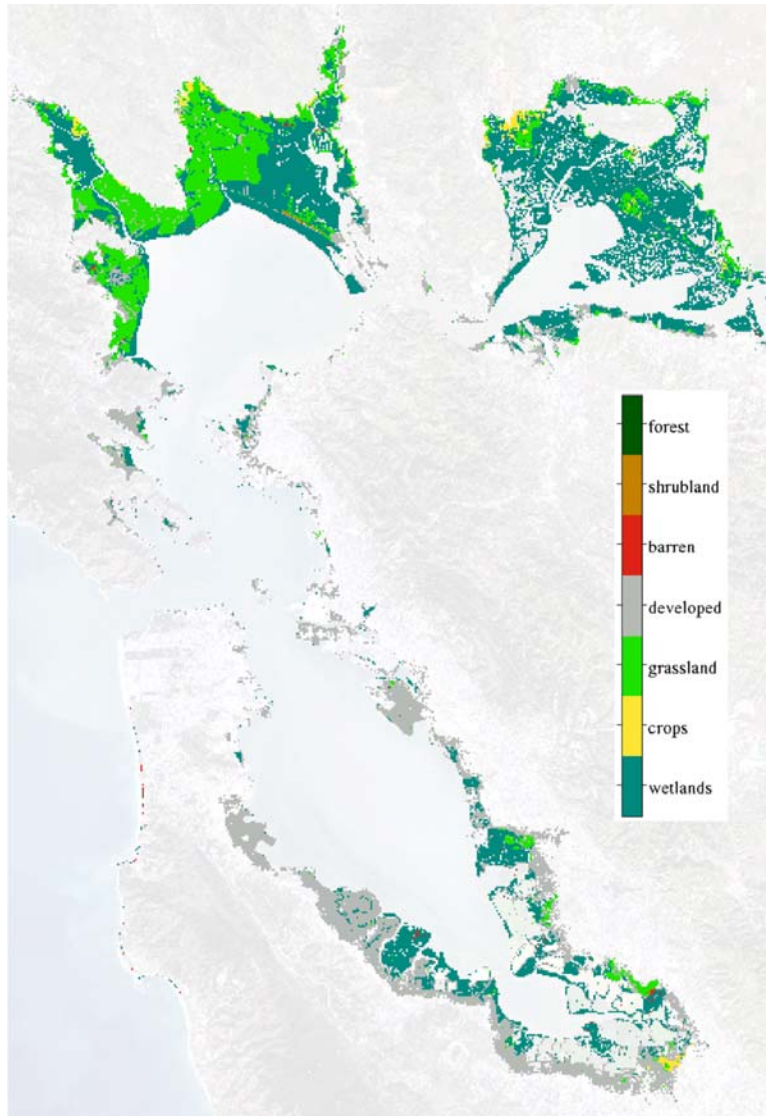


Figure 8. Land-cover types of areas vulnerable to yearly inundation as of 2099 under a projected 139 cm sea level rise

The bulk of vulnerable areas are composed of the wetlands and grasslands in North Bay (Figure 8). However, most *newly* vulnerable areas as a result of sea level rise are the developed areas surrounding Central and South bays (cf. Figure 5). These also constitute the vulnerable areas of greatest potential economic loss.

Figures 9 and 10 show close-ups of Figure 5 for North and Central/South bays, respectively, again portraying areas potentially inundated by one-year recurrence levels for present-day and projected 2099 conditions under a 139 cm sea level rise.

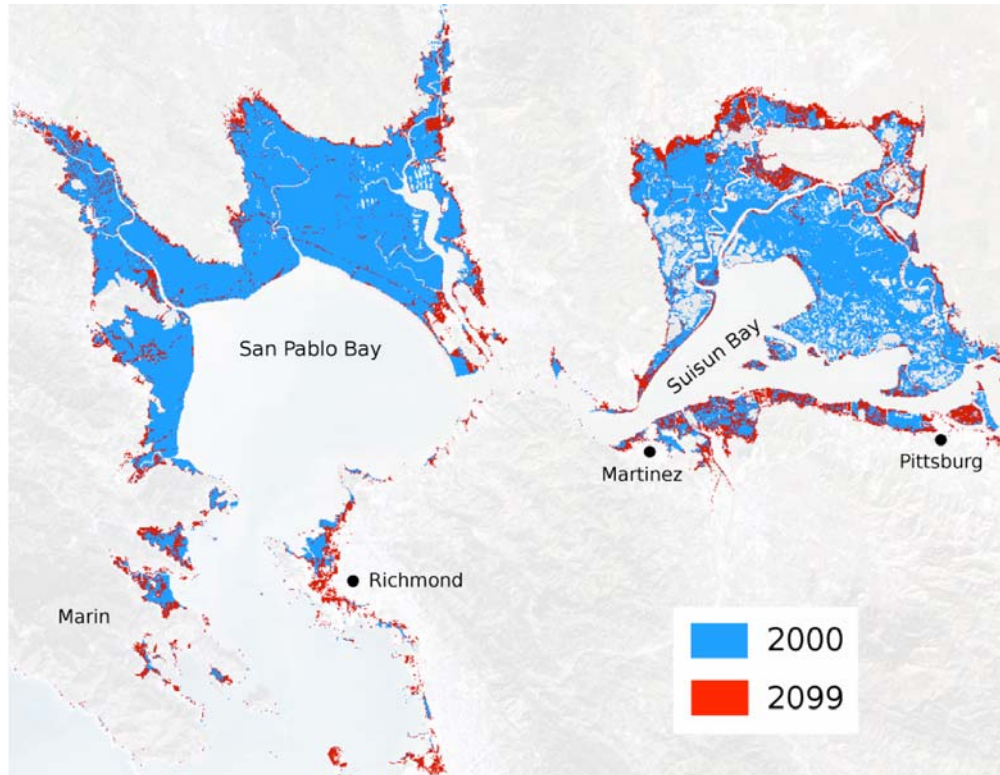


Figure 9. North Bay areas inundated or vulnerable to inundation by average yearly high water levels for present-day and projected 2100 conditions

Another key question is whether existing wetlands and shallow-water habitat would be able to accrete sediment and organic matter quickly enough to keep up with rising sea levels and maintain their position in the tidal range (e.g., Orr et al. 2003). For the wetlands alone, this would require over half a billion cubic meters of material (organic+sediment), or an average of 5.4 million cubic meters per year for the 139 cm rise portrayed here². According to estimates by Schoellhamer et al. (in: SFEI 2005), sediment input to the Bay from local sources averages 0.9×10^6 Mg/year, while the input through the Delta is about 0.8×10^6 Mg/year, though there is also evidence that this latter supply of sediment has been in decline (Wright and Schoellhamer 2004). Taken together, local and Delta inputs of sediment average 1.7×10^6 Mg/year; depending on the density estimate used (D. Schoellhamer, personal communication), this amounts to roughly 1.5×10^6 — 3.2×10^6 m³/year, considerably less than the 5×10^6 m³/year that would be needed under the CCSM3-A2 scenario. Some of the difference will be made up by marsh growth. Research is also being done to assess historical and potential future rates of organic matter accretion in the Bay region, but estimates are not yet available (J. Drexler, personal communication).

There is evidence that, at least in some parts of the Bay, wetlands are capable of keeping pace with even higher rates of relative sea level rise. In far South Bay, rates of sedimentation and

² Corresponding to a 139 cm rise over the total of 390 km² wetlands vulnerable to a one-year flood in 2099.

marsh growth were shown to have been sufficient to allow salt marshes to compensate for an estimated one meter of subsidence due to groundwater extraction over only a few decades (Patrick and DeLaune 1990; Watson 2004). However, far South Bay has been shown to be a particularly strong depositional environment relative to other areas of San Francisco Bay (Foxgrover et al. 2004; Jaffe and Foxgrover 2006). Another possibility is the creation of new wetlands as a result of landward “migration,” though in the highly developed Bay region this possibility is generally limited.

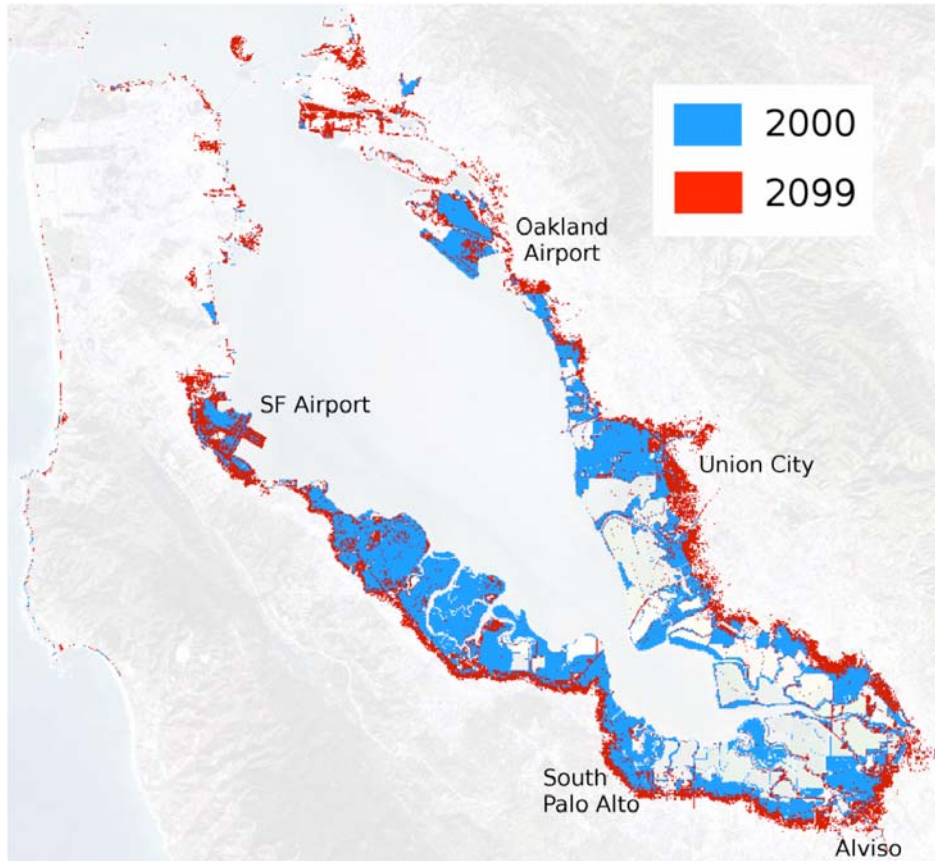


Figure 10. Central and South Bay areas inundated or vulnerable to inundation by average yearly high water levels for present-day and projected 2100 conditions

Other key areas of concern in Figure 9 are the municipal and industrial areas that are not vulnerable now but would be under this future scenario. These areas (in red) along the Martinez-Pittsburg corridor, the Richmond peninsula, and in eastern Marin are developed areas that would require some new levees and additions to existing levees in order to maintain flood protection.

In Central and South bays (Figure 10), a key feature is the ring of developed areas that would be newly vulnerable to inundation under the 139 cm scenario (the red periphery). Many of these areas are already behind levees; they simply represent lands that are not currently at risk if these levees breached but would be at risk under the future scenario. Nearly all municipalities

adjacent to South Bay (or adjacent to wetlands adjacent to South Bay) face this risk to some degree. Other areas such as the San Francisco International Airport are not currently leveed but would need to be.

A primary concern in Central and South Bays is that pressure on existing levees, and thus the risk of breaches, would be greatly increased. As sea level rises, the potential for overtopping would also increase. As in the North Bay, existing levees would need to be raised and fortified and many new levees would need to be constructed. Also as in the North Bay, the survival of existing and future restored wetlands (i.e., the Salt Ponds Restoration Project) will depend on the ability of these wetlands to accrete material quickly enough to keep pace with sea level rise. If the wetlands of South Bay were submerged by rising water levels, one consequence would be that wave energy would be less attenuated and erosional forces against upland levees would increase.

4.0 Discussion

The main features of inundation in San Francisco Bay associated with potential high-end sea level rise have been presented here. It should be emphasized that this is a scenario, not necessarily a reliable prediction. From this analysis, some major concerns associated with sea level rise can be inferred—survival of existing wetlands and shallow-water habitat, inundation of currently unprotected developed areas, increased risk of failure and overtopping of existing levees, and increased consequences of such failures as more areas become vulnerable are all real dangers. However, many other complications could also occur as sea level increases. For example, sanitation districts around the estuary are concerned that as sea level rises, seawater could backflow into their drainage systems causing local flooding and sanitation problems. The risks of such problems occurring will increase with sea level rise, but are also associated with specific events within a given year. For example, the largest events are most likely to occur during winter storms, particularly those coinciding with a spring tide. El Niño events also lead to higher water levels and increased risk.

The projected changes also have numerous implications for those living in this region. Municipal planners will need to carefully consider the increasing risks of development in low-lying areas. Changing recurrence levels will require that flood insurance maps be redrawn periodically. Local groundwater pumping will need to continue to be carefully managed to avoid subsidence. Transportation infrastructure will be threatened. Economic implications of these and other changes are discussed in the concurrent report by Heberger et al. (2008).

As mentioned in the “Data and Methods” section, these results are not limited to the particular scenario studied. The A2 emissions scenario evaluated here represents higher greenhouse gas emissions in the future (www.grida.no/climate/ipcc/emission), and as such is among the least optimistic of possible futures, resulting in projections of large warming (4.5°C) and sea level rise (139 cm) by 2100. For comparison, estimates of sea level rise under the most optimistic of scenarios, representing lower greenhouse gas emissions, range from 45–70 cm by 2100 (Moser et al. 2008). Referring to Figure 3, these values correspond to the conditions in 2050–2065 under the A2 scenario evaluated here. This means that under the most optimistic scenarios, the changes presented here as occurring by 2050–2065 would not occur until 2100. For example, referring to Figure 6, we see that even under the most optimistic scenario, in 2100 the 1-year peak event would nearly equal today's 100-year peak event.

Understanding and successfully adapting to these changes will require a fuller knowledge of the likely consequences and the types of actions required. A good example of a gap in our current knowledge is the need for a better understanding of the adaptability of existing and restorable wetlands and the dependence of the survival of these wetlands on the Bay's sediment budget. Another very important missing piece of information is a better characterization of levee heights and their recent changes due to subsidence or uplift, and an associated regional database.

Inundation data layers from this project are publicly available at <http://cascade.wr.usgs.gov> in the hope that the high-resolution regional data produced for this analysis will prove useful for other regional and local studies and planning efforts. Future work will incorporate bathymetric data and address, among other issues, potential shifts in tidal zones and changes in shallow-water habitat.

5.0 References

- Cayan, D. R., P. D. Bromirski, K. Hayhoe, M. Tyree, M. D. Dettinger, and R. E. Flick. 2008. "Climate change projections of sea level extremes along the California coast." *Climatic Change* **87** (Suppl 1):S57–S73, doi:10.1007/s10584-007-9376-7.
- Cayan, D. R., M. Tyree, M. D. Dettinger, H. Hidalgo, and T. Das. 2009. California Climate Change Scenarios and Sea Level Rise Estimates for California 2008 Climate Change Scenarios Assessment. California Climate Change Center. In preparation.
- Cheng, R. T., V. Casulli, and J. W. Gartner. 1993. "Tidal, Residual, Intertidal Mudflat (TRIM) Model and its Applications to San Francisco Bay, California." *Estuarine, Coastal and Shelf Science* **36**:235–280.
- Cheng, R. T., and J. W. Gartner. 1984. *Tides, tidal and residual currents in San Francisco Bay California - results of measurements, 1979–1980*. U.S. Geological Survey Water-Resources Investigations Report No. 84-4339.
- Church, J. A., N. J. White, R. Coleman, K. Lambeck, and J. X. Mitrovica. 2004. "Estimates of the regional distribution of sea level rise over the 1950–2000 period." *J. Climate* **17**:2609–2625.
- Church, J. A., and N. J. White. 2006. "A 20th century acceleration in global sea-level rise." *Geophys. Res. Lett.* **33**: L01602, doi:10.1029/2005GL024826.
- Coons, T., Soulard, C. E., and N. Knowles. 2008. *High-resolution digital terrain models of the Sacramento/San Joaquin Delta Region, California*. U.S. Geological Survey, Data Series 359 <http://pubs.usgs.gov/ds/359>.
- Fisher, R. A., and L. H. C. Tippett. 1928. "Limiting forms of the frequency distribution of the largest or smallest member of a sample." *Proceeding of Cambridge Philosophical Society* **24**:180–190.
- Flick, R. 2003. "Trends in United States tidal datum statistics and tide range." *Journal of Waterway, Port, Coastal and Ocean Engineering* **129**(4):155–164.

- Foxgrover, A. C., S. A. Higgins, M. K. Ingraca, B. E. Jaffe, and R. E. Smith. 2004. *Deposition, erosion, and bathymetric change in South San Francisco Bay: 1858–1983*. U.S. Geological Survey Open-File Report 2004-1192, 25 pp. <http://pubs.usgs.gov/of/2004/1192>.
- Foxgrover, A. C., and B. E. Jaffe. 2005. *South San Francisco Bay 2004. Topographic Lidar Survey: Data Overview and Preliminary Quality Assessment*. U.S. Geological Survey Open-File Report 2005–1284.
- Gleick, P. H., and E. P. Maurer. 1990. *Assessing the Costs of Adapting to Sea-Level Rise: A Case Study of San Francisco Bay*. Pacific Institute Report. www.pacinst.org/reports/sea_level_rise/index.htm.
- Goals Project. 1999. *Baylands Ecosystem Habitat Goals. A report of habitat recommendations prepared by the San Francisco Bay Area Wetlands Ecosystem Goals Project*. U.S. Environmental Protection Agency, San Francisco, Calif. / S.F. Bay Regional Water Quality Control Board, Oakland, Calif.
- Heberger, M., Cooley, H., Herrera, P., and P. H. Gleick. 2008. *The Cost of Adapting to Sea Level Rise along the California Coast and in the San Francisco Bay*. California Energy Commission, PIER Energy-Related Environmental Research. Draft paper.
- Hidalgo, H., M.D. Dettinger, and D. R. Cayan. 2008. *Downscaling with constructed analogues—Daily precipitation and temperature fields over the United States*. California Energy Commission PIER report.
- IPCC. 2001. *Climate Change 2001, the Third Assessment Report (AR3) of the United Nations Intergovernmental Panel on Climate Change (IPCC)*.
- IPCC. 2007. *Climate Change 2007, the Fourth Assessment Report (AR4) of the United Nations Intergovernmental Panel on Climate Change (IPCC)*.
- Jaffe, B. E., and A. C. Foxgrover. 2006. *Sediment Deposition and Erosion in South San Francisco Bay, California from 1956 to 2005*. U.S. Geological Survey Open-File Report 2006–1262, 24 pp. <http://pubs.usgs.gov/of/2006/1287>.
- Knowles, N., and D. Cayan. 2002. "Potential effects of global warming on the Sacramento/San Joaquin watershed and the San Francisco estuary." *Geophysical Research Letters* **29**:38-1–38-4.
- McKee, L. J., N. K. Ganju, and D. H. Schoellhamer. 2005. "Estimates of suspended sediment entering San Francisco Bay from the Sacramento and San Joaquin Delta, San Francisco Bay, California." *Journal of Hydrology* **323**:335–352.
- Mitasova, H., and J. Hofierka. 1993. "Interpolation by Regularized Spline with Tension: II. Application to Terrain Modeling and Surface Geometry Analysis." *Mathematical Geology* **25**:657–667.
- Moser, S. C., D. R. Cayan, and G. Franco. 2008. *The Future Is Now—An Update on Climate Change Science, Impacts, and Response Options for California*. California Climate Change Center CEC PIER Report, September, 2008.

- Orr, M., S. Crooks, and P. B. Williams. 2003. "Will Restored Tidal Marshes Be Sustainable?" *San Francisco Estuary and Watershed Science* 1(1), Article 5.
- Patrick, W. H., and R. D. Delaune. 1990. "Subsidence, accretion, and sea level rise in south San Francisco Bay marshes." *Limnology and Oceanography* 35(6): 1389–1395.
- Pfeffer, W. T., J. T. Harper, and S. O'Neel. 2008. "Kinematic Constraints on Glacier Contributions to 21st-Century Sea-Level Rise." *Science* 321(5894): 1340–1343.
- Rahmstorf, S. 2007. A Semi-empirical approach to projecting future sea-level rise. *Science* 315: 368–370.
- San Francisco Estuary Institute (SFEI). 2005. *The Pulse of the Estuary: Monitoring and Managing Water Quality in the San Francisco Estuary*. SFEI Contribution 411. San Francisco Estuary Institute, Oakland, CA.
- Watson, E. B. 2004. "Changing elevation, accretion, and tidal marsh plant assemblages in South San Francisco Bay tidal marsh." *Estuaries* 27(4):684–698.
- Wigley, T. M. L. 2005. "The Climate Change Commitment." *Science* 307:5716, 1766–1769.
- Williams, P. B. 1985. *An overview of the impact of accelerated sea level rise on San Francisco Bay*. Project No. 256, for the Bay Conservation and Development Commission. Philip Williams and Associates, San Francisco, California.
- Williams, P. B. 1987. *The impacts of climate change on the salinity of San Francisco Bay*. Philip Williams and Associates, San Francisco, California. EPA Rept # EPA-230-05-89-051.
- Wright, S. A., and D. H. Schoellhamer. 2004. "Trends in the sediment yield of the Sacramento River, California, 1957–2001." *San Francisco Estuary and Watershed Science* [online serial]. 2(2), May 2004, Article 2.

6.0 Glossary

GEV	generalized extreme value distribution
IfSAR	interferometric synthetic aperture radar
LiDAR	light detection and ranging
MHW	mean high water
MLLW	mean lower-low water
NAVD88	North American Vertical Datum of 1988
NCALM	National Center for Airborne Laser Mapping
NGA	National Geospatial-Intelligence Agency
NLCD01	National Land Cover Dataset of 2001
NOAA	National Aeronautic and Atmospheric Administration

RMSE	root mean square error
SFEI	San Francisco Estuary Institute
USGS	U.S. Geological Survey